Microsystem Technologies (2021) 27:3225–3233
https://doi.org/10.1007/s00542-020-05208-7

TECHNICAL PAPER

A squared bossed diaphragm piezoresistive pressure sensor based on CNTs for low pressure range with enhanced sensitivity

Rekha Devi[1,2] · Sandeep Singh Gill[3]

Received: 17 October 2020 / Accepted: 29 December 2020 / Published online: 13 January 2021

Abstract
This paper presents Micro-Electro-Mechanical System (MEMS) diaphragm based piezoresistive pressure sensor for biomedical applications. A piezoresistive pressure sensor with a squared bossed diaphragm structure was developed for a low-pressure range. A trade-off between the deformation of the diaphragm and the stress induced in the piezo resistors on the diaphragm edge is analysis by using Carbon nanotubes (CNTs). CNTs are introduced in the sensor being a sensitivity material, responsible for wide range of pressure and sensitivity. The simulated results showed that the proposed structure was able to measure low pressure within range of 0–5 kPa with improved sensitivity and linearity. An 800-µm-wide 10-µm-thick square-diaphragm pressure sensor has also been designed and investigated for the different mender shape. It has been observed from the results that maximum sensitivity of 27.82 mV/kPa is achieved for 2-turn piezo resistor and the best non-linearity error − 0.27% FSS is achieved for 1-turn piezo resistor.

1 Introduction

Micro-Electro-Mechanical System (MEMS) is developed and popular technology. Integrated circuit (IC) processing adopted this technology for fabricating the micro-sensors for the measurement of the various process variables like pressure, distance, temperature, fluid flow, acceleration, angular velocity, and rotation, etc. (Mishra and Kumar 2019). MEMS based pressure sensor can detect the very low range of pressure in micrometers and small feature size, good performance, low power requirements, and feasible mass-production in the micromachining process (Tran et al. 2017). The measurements of intracranial pressure (ICP), intrauterine pressure (IUP), the inlet and outlet pressures of blood and intraocular pressure (IOP) have great significance for biomedical applications. The ICP and IOP are kept usually in range 0.78–1.76 kPa and 1.47–2.79 kPa, respectively. The blood pressure measurements 25.7 mm Hg, 3.43 kPa and 0.1 mm Hg in a 20 mm Hg is required like IUP. Therefore, a pressure sensor with a high sensitivity and linearity (smaller than 0.5%) in 0–5 kPa is required for monitoring biomedical applications (Hossain and Mian 2017; Huang and Zhang 2014b; Guan et al. 2016). Different principles of sensing for senor design have been considered to adapt to various environments. These principles are optical fibre grating sensor, strain gauge, piezo-capacitance, piezoelectric, resonant sensing mechanisms, and piezoresistive sensor, etc. few measuring restrictions are found in most of the principles (Niu et al. 2014). Piezoresistive pressure sensors have high sensitivity and low cost in comparison with other sensors (Sosa et al. 2015). In this paper, A Centre Squared Bossed Diaphragms (CSBD) is proposed to improve Non-Linearity and sensitivity of the pressure sensor. CNTs use as piezoresistor elements because of strong sensing capabilities, and as centred bossed to concentrate the more stress at the edges of the diaphragms thus obtain the good linearity at the same thickness.

2 Piezoresistive pressure sensor

The piezoresistive pressure sensor consists of four piezoresistors, which are arranged in a configuration of the Wheatstone bridge to measure the output voltage. When no pressure is applied, the bridge is in a balanced state, i.e.,

✉ Rekha Devi
erekha0723@gmail.com

[1] IKG Punjab Technical University, Jalandhar, India

[2] Chandigarh University, Mohali, India

[3] National Institute for Technical Teachers Training and Research Chandigarh, Chandigarh, India

Vout = 0 V because each piezo resistor has equal resistance. This principle has the advantages of good accuracy, higher piezoresistance coefficient, simple signal transduction and easy fabrication (Jakati et al. 2016; Lu et al. 2007; Xu et al. 2017). According to the effect with the applied pressure the diaphragm of the pressure sensor would deflect and cause the change in piezoresistor's values. There are few fundamental factors to be considered for improvement of the sensitivity and linearity of the pressure sensor, first the placement of piezoresistors need to be done at the maximum stress region. In the case of the square diaphragm pressure sensor, the maximum stresses are produced at the centre of each edge of the diaphragm. Hence the four piezo resistors are pledges of the diaphragms as shown in Fig. 1. The width of centre boss need to be optimized to address the design limitations of nonlinearity errors. The centre boss is usually moulded by selectively design from the backside of a wafer with the sidewalls of 54.7.

Second the shape, thickness, material, dimensions of the diaphragms, thirdly the doping concentration of both piezo resistor and diaphragm play very effective roles in the sensitivity of the low-pressure sensor. The performance of the sensor can also improve by changing the position and shape of the piezo resistors.

2.1 Nano material as sensing elements

Silicon Carbide, Silicon, Germanium, polysilicon, CNTs, bismuth sulfide (Bi_2S_3) and Graphene materials have a piezoresistive effect (Zhu et al. 2013; Song et al. 2020b; Bala and Khosla 2018; Ali et al. 2017). Compared to bulk silicon, silicon nanowires have seven times the piezoresistive effect (Shaby et al. 2015; Kim et al. 2009). The materials with the piezoresistive effect can be used as a transducer and produced an electrical signal as a function of applied mechanical stress (Tran et al. 2017). Sensitive materials such CNTs affecting the performance of pressure sensors due to its remarkable electronic properties (Wang et al. 2020).

The foremost properties of CNTs are that bandgap of the CNT material is inversely proportional to the diameter of the tube, Single-walled carbon nanotube (SWCNT) and Multi-walled nanotube (MWCNT) are two basic structure of the CNT showed in Fig. 2. SWCNTs are an imperative because they exhibit electric properties that are not shared by MWCNT (Aqel et al. 2012). The basic principle of CNT nano sensor has arrived from the fact that radial deformation and electrical transition induced in armchair SWNT with hydrostatic pressure (Li et al. 2017). MWCNTs have several layers in concentric cylinders with diameter from 3 to 30 nm rolled one inside others and they were closed at both ends as in Fig. 2b. CNTs behave like a metallic as well as semiconductor depending on chiral vector as $c = na_{1+} ma_2$ here (m, n) is chiral number and a_1 and a_2 is unit vector.

In fig 3a, the circumference of CNT is $= |C| = \sqrt[a]{(n^2 + mn + m^2)}$. Here a is unit vector. The diameter ($d = \frac{c}{\pi}$) of CNTs depends on the size of the catalyst particles (Gupta et al. 2019). Variation in strain effect the band gap as given in (1), here v is passion ratio, ε is axial strain, γ torsional strain, or the hopping integer ($\sim$ 2.6 Ev). The resistance of the CNTs can be occurred due to electron transport due to thermal activation as given below in Eq. (2)

$$\Delta E_{gap} = \sin(2p+1)3t_o[(1+v)\varepsilon\cos 3\theta + \gamma\sin 3\theta)] \quad (1)$$

$$R = R_C + \frac{1}{|t^2|}\frac{h}{8e^2}\left[1 + \exp\left(\frac{E_g}{KT}\right)\right] \quad (2)$$

$$E_g = E^o_{gap} + \frac{dE_{gap}}{d\varepsilon}\epsilon \quad (3)$$

$|t^2|$ is the electron transmission probability, R_c presents the contact resistance in series, h denotes the plank's constant, T is temperature, electron charge is represented by e, k provides Boltzmann's constant, E_g is bandgap energy that depends upon the strain Eq. (3) for a semiconducting CNTs is $E^o_{gap} = \frac{t_o a^2}{4d^2}$. It is concluded from the second equation that when strain is applied changed CNTs resistance which

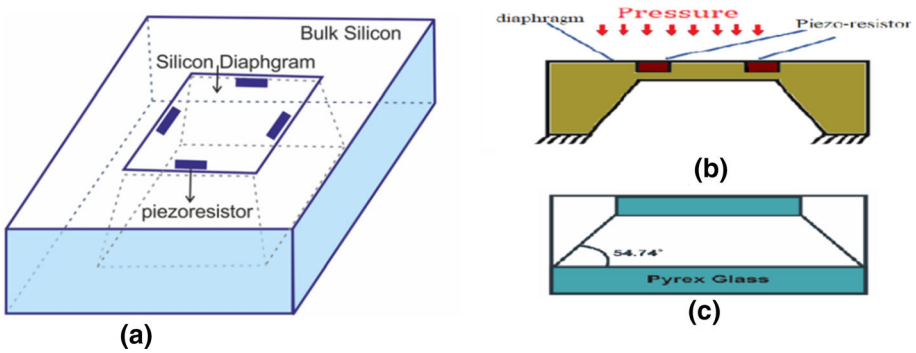

Fig. 1 **a** Schematic of a piezoresistive pressure sensor (top view), **b** cross sectional schematic of the pressure sensor

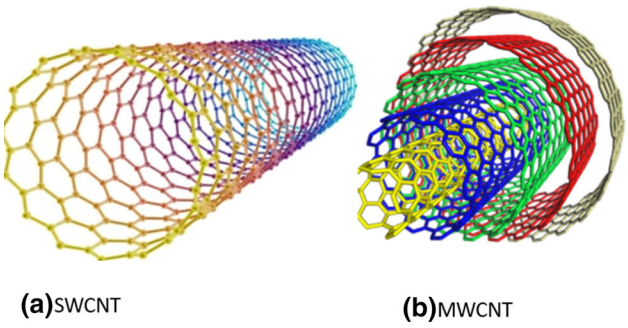

Fig. 2 **a** Internal view of single wall carbon nanotube (SWCNT) and **b** Multiwall nanotube (MWCNT) (Gupta et al. 2019)

building it as best material for piezoresistive (Katageri and Sheeparamatti 2015).

2.2 Different structure

The designing of a new efficient structure and optimize the locations of the piezo resistor on the diaphragm, the dimensions of the piezo resistors and diaphragm, structure of the diaphragm, and the shapes of components. This approach has been established for the designing of the several diaphragms structures (Tran et al. 2017). A pressure sensor of combined peninsula island with a bossed diaphragm structure with dimensions 3500 × 3500 um^2 was designed by Xu et al. the nonlinearity of 0.33% FSS and a sensitivity of 0.066 mV/V/Pa was reported (Tran et al. 2018). Four Peninsulas with a centre Bossed diaphragm structure was demonstrated at low pressure to obtain high sensitivity and linearity (Huang and Zhang 2014a) peninsula-island combined with a bossed diaphragm structure was proposed to diminish the trade-off between nonlinearity and sensitivity for ultra-low pressure (Xu et al. 2016). A peninsula–island combined with the bossed diaphragm was tested with a non-linearity of 0.42% FS and sensitivity of 66 μV/V/Pa (Zhao et al. 2016). Crossed beam on the top of silicon membrane was etched for stress concentration to the detection pressure (0.5–40 kPa) (Yu and Huang 2015). The pressure sensor was designed using four grooves with a working range of 0–500 Pa and had a high sensitivity of 0.06 (Xu et al. 2017). A shuriken-structured diaphragm (SSD) was design to improve both linearity and sensitivity (Guan et al. 2016).

3 Small deflection diaphragm theory

To design a pressure sensor, mostly the conventional square diaphragm flat membrane is used for high linearity and accuracy. The square diaphragm has other meaning full advantages are there like low nonlinearity and simultaneous high sensitivity as well as decrease the influence of process fluctuations on the output characteristics of the pressure sensor (Li et al. 2020). The performance of sensor is measured maximum linearity and produced stress. Smaller diaphragm with same thickness offered high linearity and poor sensitivity and vice versa and true for larger diaphragm vice versa. Based on theory of electricity, the maximum stress induced in diaphragm is calculated by the given Eq. (4) (Li et al. 2017).

$$stress(\sigma) = 0.308P\left(\frac{L}{h}\right)^2\left(1-\mu^2\right) \tag{4}$$

where P is the applied pressure, μ is the passion ratio, L/h is the length to thickness ratio of square diaphragm. To obtain more stress this ratio is to improve. When the deflection of the squared diaphragms exceeds the certain value compared to its thickness, the large deflection theories work, and then there will be nonlinear relation of defection with applied pressure. A combination method was developed to resolve the large deflection. Applied pressure P is divide into bending stress and shearing stress ($P = P_a + P_{b)}$ and small deflection theory was used to derive P_a by using Eq. (5) Large deflection theory was used to derive P_b by using Eq. (6). Both the equations are separately deduced and at end combined together Eq. (7) (Suja et al. 2015).

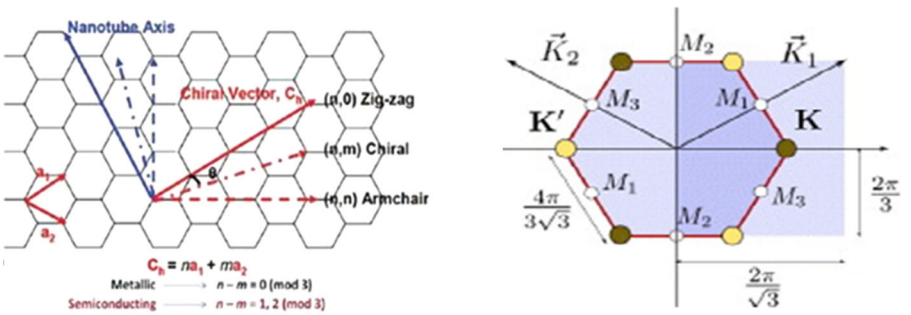

(a) Chiral vector **(b)** The first Brillouin zone (BZ))

Fig. 3 **a** Chiral vector of CNTs and **b** the first Brillouin zone (BZ) of graphene

$$P_a = 71.3\frac{\omega E h^3}{L^4} \tag{5}$$

$$P_b = 31.1\frac{\omega^3 E h}{L^4} \tag{6}$$

$$\frac{PL^4}{Eh^4} = 71.3\left(\frac{\omega}{h}\right) + 31.1\left(\frac{\omega}{h}\right)^3$$

or

$$\frac{PL^4}{Eh^4} = \frac{4.2}{(1-\mu^2)}\left(\frac{\omega}{h}\right) + \frac{1.58}{(1-\mu^2)}\left(\frac{\omega}{h}\right)^3 \tag{7}$$

From Eq. (7) relative load is $\frac{PL^4}{Eh^4}$ and the reative deflection is the ratio of deflection to thicknes of diaphragm as slowen in Fig. 4.

It can be seen from the large deflection curve, that when the relative deflection is goes beyond 0.2, the relationship of deflection and load is no longer remain linear. The deflection of diaphragm must be less than 1/5th of the thickness of diaphragm according to small deflection theory for obtaining low nonlinearity.

4 Design of the centre squared bossed diaphragms (CSBD)

CSBD with piezo resistors was proposed to measure pressure ranging from 0 to 5 kPa, shown in Fig. 5a. Four piezo resistors are connected in such a way to form wheat stone bridge at centre of the edges of the diaphragms. The rigidity of the diaphragm needs to be increased for avoid deformation of the diaphragm (Huang and Zhang 2014a; Zou et al. 2017). The centre bosses on the backside are added to set the diaphragm, as shown in Fig. 5b. This structure relieved the discrepancy between the linearity error and sensitivity. In the proposed structure the side length (L = 800 μm) and the thickness (h = 10 μm) of the diaphragm has been taken for high sensor outputs. The

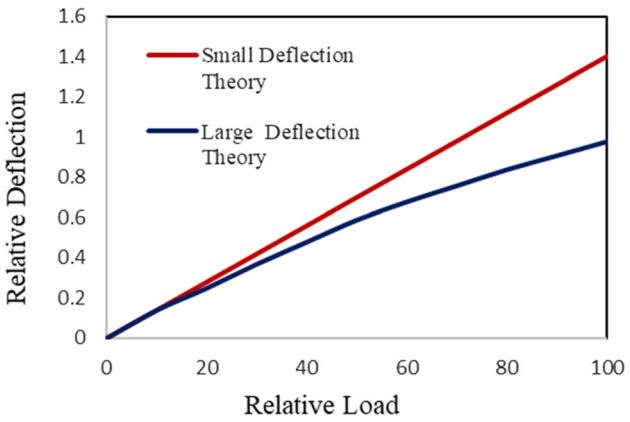

Fig. 4 Normalized deflection for small and large theory

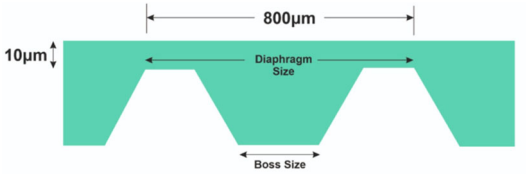

(a) Cross-section of bossed diaphragm sensor structure

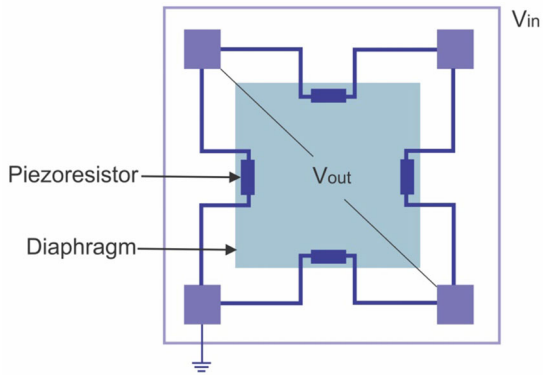

(b) Arrangement of piezoresistor as aWheat stone bridge

Fig. 5 a Cross-section of bossed diaphragm sensor structure. **b** Arrangement of piezoresistor as a wheat stone bridge

distribution of stress intensity for the CSBD diaphragm has been investigated under 5000 Pa pressure.

5 Structure analysis and simulation results

5.1 Diaphragm deformation

The maximum deformation of the diaphragm is a function of diaphragms geometry and shape as given by Eq. (8) to achieve good sensitivity a thinner diaphragm is preferred. However, as the thickness reduces, the stiffness/stability is also diminishing.in order to maintain the linearity canter bossed is added (Meena et al. 2017).

The novel structures have been designed based on a local stiffening of the membrane to reduction in nonlinearity. The flexural stiffness is given in Eq. (8) (Song et al. 2020a; Kumar and Tanwar 2020; Zhang et al. 2014).

$$\omega = \frac{0.0159P(1-\mu^2)L^4}{Eh^4} \tag{8}$$

$$D = \frac{Eh^2}{12(1-\mu^2)} \tag{9}$$

D is flexural stiffness, E defines the Young modulus; μ represented Poisson ratio (Zhao et al. 2016). It is analyzed from the pressure deformation response that the squared diaphragm provides linear deformation performance over the specified pressure range. Figure 6 shows simulation

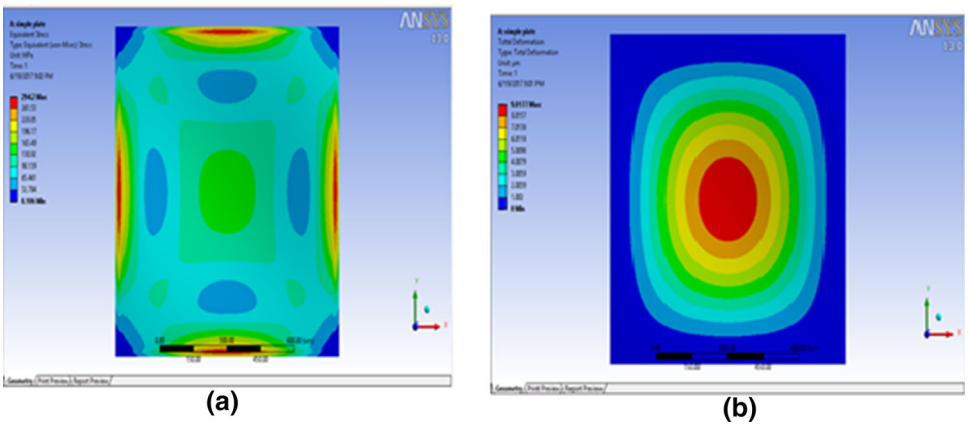

Fig. 6 Simulation results for **a** stress and **b**, deformation at applied pressure

results of stresses and displacement for CSBD structure. In addition, at the center of the diaphragm displacement is maximum as shown in Fig. 6a. Maximum stress is located at the center (red area) of the edge on the diaphragms given in Fig. 6b. Therefore, two piezoresistive gauges required to be placed at the center of the line with (x = 0; y = ± 400 µm) and the other two gauges must be situated in the middle of the edges respectively. For example, their center was at the points (x = ± 400 µm, y = 0). According to small deflection theory, the maximum deformation should be less than 1/5 of the diaphragm thickness $\omega_{max} \leq 0.2\ h.$ accordingly, if the thickness is $h = 10$ µm, it allowed a maximum deformation 2 µm. Figure 7a shows the maximum equivalent stress and (b) total deformation at the centre of the diaphragm for variation in diaphragm size. It has been determining that stress and deflection increases by large diaphragm and the sensor have good sensitivity due to more deformation, but linearity is almost vanished.so to obtain better results for sensitivity and the linearity, the centre of the diaphragm should be stiffening. Squared bossed is added at the centre to increase the stiffness of the diaphragm. Comparison of total deformation of different bossed size and bossed with CNTs Material in response of applied pressure ranging from 0 to 5000 Pa showed in Fig. 7c and analyzed from that with increased bossed size, maximum deformation at center is going to decreased and bossed with cnt material provide less deformation at the center and stiffen the diaphragm at the center.

5.2 Final output of the sensor

Four piezoresistors in Wheatstone bridge, (R_1 and R_3) are placed in longitudinal and R_2 and R_4 are in transverse direction. N-type silicon material is used for designing of the diaphragms and all the piezoresistor are of CNT material. The longitudinal and transverse stress is induced on all the piezoresistors with the applied pressure on the diaphragms. σx_1 is longitudinal stress and σy_1 is transverse stress on R_1 and R_3 similarly σy_2 is longitudinal stress and σx_2 is transverse stress on R_2 and R_4. The cross-sectional area, the length and resistivity of the resistor are related to the resistance. The internal resistance of the piezoresistor will changed with these stresses. The change in length and cross section area are the dimensional effect and can be neglected. The change in resistivity is the physical effect and related to the transversal and the longitudinal (Yu and Huang 2015). Some positive change ΔR_1 with the resistance R_1–R_3 and same negative change ΔR_2 with the resistance R_2–R_4 (Gupta et al. 2019). The overall change in the resistance is represented by the Eq. (10) where π_{44} is the piezoresistive coefficient. Out the output voltage of the Wheatstone bridge circuit can be calculated in terms of input voltage V_{in} is 5 V.

$$\begin{aligned}\frac{\Delta R_3}{R_3} &= \frac{\Delta R_1}{R_1} = \left(\frac{\pi_{44}}{2}\right)(\sigma x_1 - \sigma y_1) = \left(\frac{\pi_{44}}{2}\right)\sigma_{LT1} \\ \frac{\Delta R_4}{R_4} &= \frac{\Delta R_2}{R_2} = \left(\frac{\pi_{44}}{2}\right)(\sigma x_2 - \sigma y_2) = \left(\frac{\pi_{44}}{2}\right)\sigma_{LT2}\end{aligned} \tag{10}$$

$$V_{out} = V_{in}\frac{\left(\frac{\Delta R_1}{R_1} - \frac{\Delta R_2}{R_2}\right)}{2 + \frac{\Delta R_1}{R_1} + \frac{\Delta R_2}{R_2}} = V_{in}\frac{\sigma \mathrm{LT1} - \sigma \mathrm{LT1}}{\frac{\pi_{44}}{2} + \sigma \mathrm{LT1} + \sigma \mathrm{LT1}} \tag{11a}$$

$$V_{out} = P\frac{a_2}{h_2}(1 - \nu)\pi_{44}V_{in} \tag{11b}$$

Overall output voltage of the bridge is V_{out} represented by Eqs. (11a, 11b) and that is prepositional to the applied Pressure P, ratio of diaphragm's length (L) to weight (h) and given input.

5.3 Sensor sensitivity and linearity

The trade-off between Linearity and sensitivity conflicts at low-pressure. Since sensitivity of a sensor is proportional to the ratio of length and thickness of diaphragms (L/h). However, the nonlinearity found to be increased with L/h ratio. To achieve an enhanced sensitivity and attenuate the

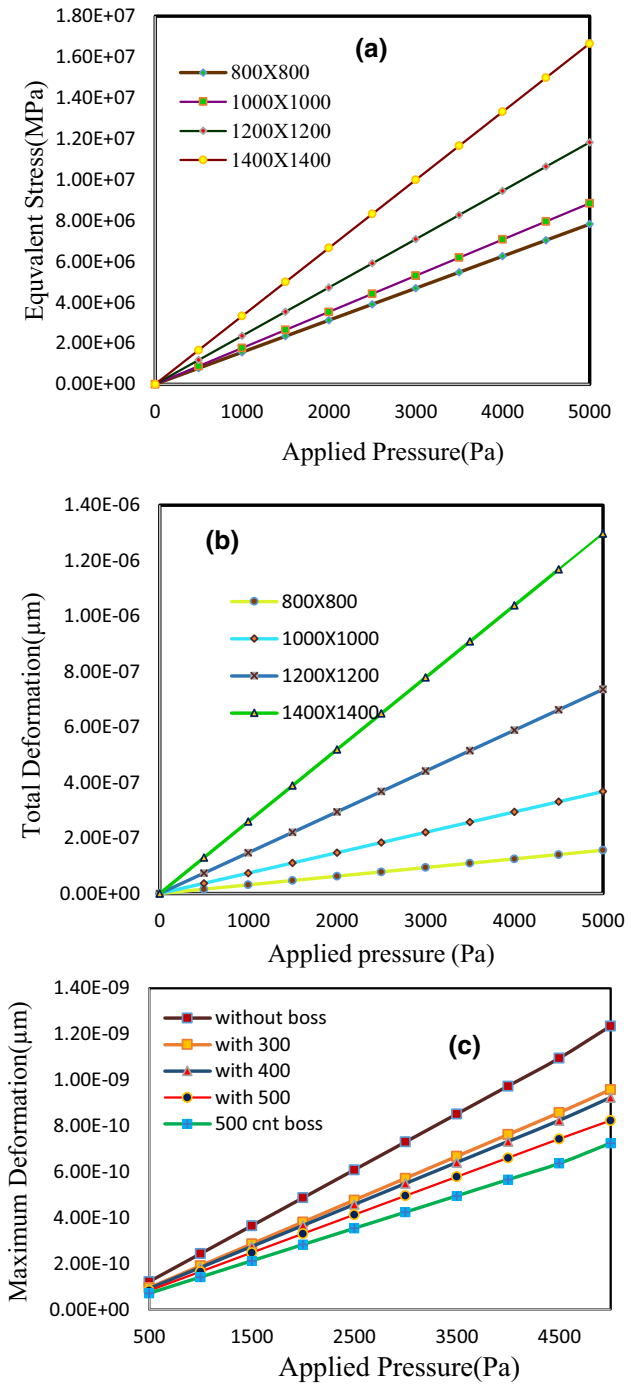

Fig. 7 **a** Maximum equivalent stress and **b** maximum deflection in the centre of the diaphragm for different diaphragms dimensions, **c** maximum deflection in the centre of the diaphragm for different bossed size

contradiction between the Linearity and sensitivity simultaneously, many structurally sensitive membranes were developed. (Li et al. 2018).

The sensitivity, which is the most important factor reflecting the capability of the proposed were developed pressure sensor, can be defined as

$$S = \frac{\left[V_{out}(P_{\max}) - V_{out}(P_{min})\right]}{(P_{max} - P_{min})} = \frac{V_{FS}}{(P_{max} - P_{min})} \quad (12)$$

where P_{max} and P_{min} are the maximum and minimum applied pressure, $V_{out}(P_{\max})$ and $V_{out}(P_{\min})$ are calculated output voltage at P_{max} and P_{min}, respectively and $V_{FS} = V_{out}(P_{\max}) - V_{out}(P_{min})$ is the Full -Scale Span (FSS).

$$NL_t = 100\% * \left[V_{out}(P_t) - (P_t)\frac{V_{out}(P_{max})}{P_{max}}\right] / \frac{V_{out}}{(P_{max})} \quad (13)$$

where P_t is pressure measured at tested points. $V_{out}(P_{\max})$ is the FSS output voltage at maximum input pressure $(P_{\max})$. Hence the nonlinearity can be either negative or positive depending on the calibration point.

The sensitivity(S) of the sensor under 5000 Pa were simulated and are shown in Fig. 8a and b. Compared with different bossed size and it was found that with increased diaphragms thickness the sensitivity is decreased and increased with improved bossed size.

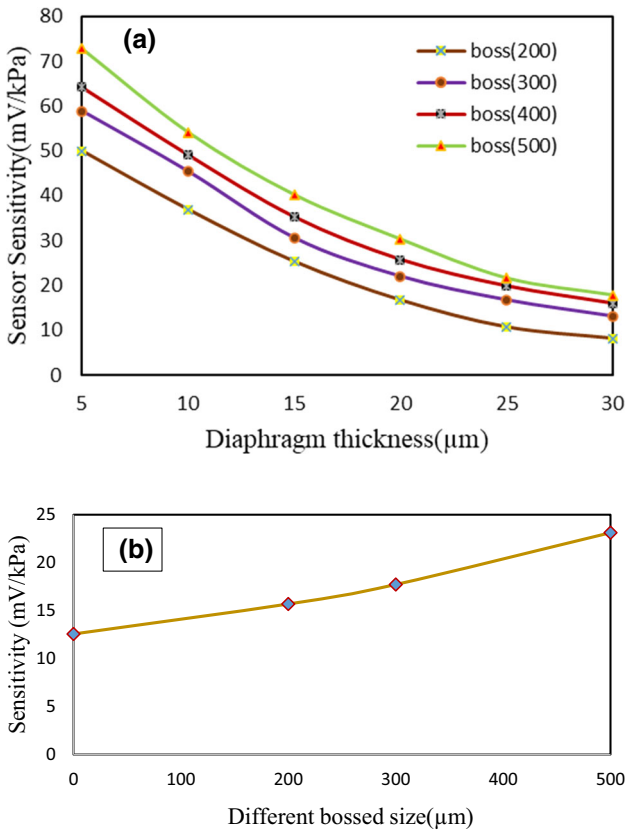

Fig. 8 **a** Sensor sensitivity as a function of **a** diaphragm thickness, **b** different bossed size

6 Different meander configurations

Three different types of piezo resistors were introduced in the design as shown in Fig. 9. The length of the all piezoresistive bars should be equal. To calculate the response of pressure sensor used by various designs of piezo resistor, the average transverse and longitudinal stresses are derived by Finite element analysis (FEA). The output of the pressure sensor with various designs can be computed from the stresses and piezoresistive coefficients of CNT by using Eq. (11). However, in Eqs. (12) and (13), defines the non-linearity error and sensitivity.

The input voltage of the sensor V_{in} is fixed at 5 V. Figures 10 and 11 demonstrated the relationship of the applied pressure (0–5000 Pa) versus output voltages and non-linearity errors for dissimilar designs of piezoresistors likes design I with 0-turn, design II with 1-turn, design III with 2-turn and design IV with 3-turns. It was observed that the changes in sensitivity and nonlinearity causes due to shifting of resistors position. Linearity and sensitivity are mainly function of piezoresistor locations. In design III piezoresistors are breaks into two turns to increase the average stress over the four piezoresitors.

The design III found to have a maximum sensitivity of 27.82 mV/kPa. Design II gives the tremendous non-linearity error of − 0.27% FSS. Table 1 represented the comparison of sensitivity and linearity of the pressure sensor. It has been seen from the results that the design III can be the considered for the proposed sensor.

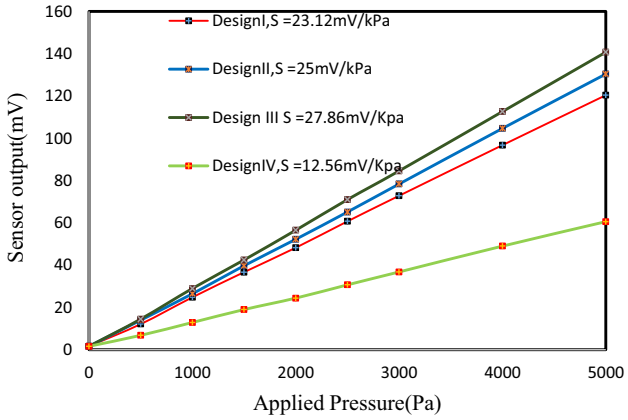

Fig. 10 Simulated sensor output of four different piezoresistor configurations

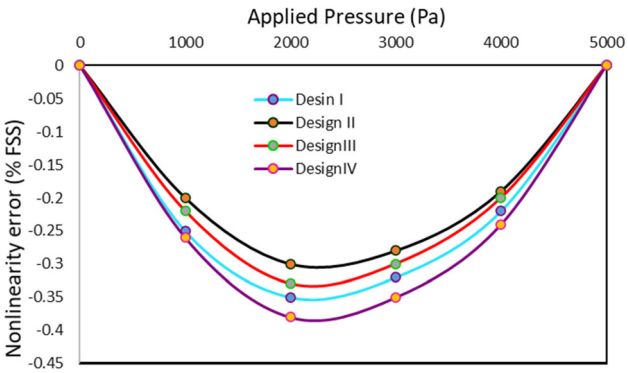

Fig. 11 Nonlinearity error for different of four different piezoresistor configurations

7 Conclusion

In this work, a squared bossed diaphragm piezoresistive pressure sensor has been designed and analysed for low pressure range. The simulation results show that the proposed structure stiffened the diaphragm to improve the linearity and developed more strain energy in the SCR to assure the higher sensitivity. Further, CNTs based piezoresistive pressure sensor provides tremendous performance. The sensitivity and linearity of the piezoresistive pressure sensors have also been studied for square-shape diaphragms. It has been found that the different configuration of piezoresistors and the thickness (h) of the diaphragm affects the characteristics of sensitivity and nonlinearity error. In addition, four different meander configurations are applied to analyse the linearity and sensitivity. The simulation results shows that the 2-turn meander configuration provides ultimate sensitivity of 27.82 mV/kPa and the 1 turn meander configuration is found to give the least non-linearity of 0.5051%. Therefore, either of these meander configurations may be considered for the improvement of overall performance of the sensor.

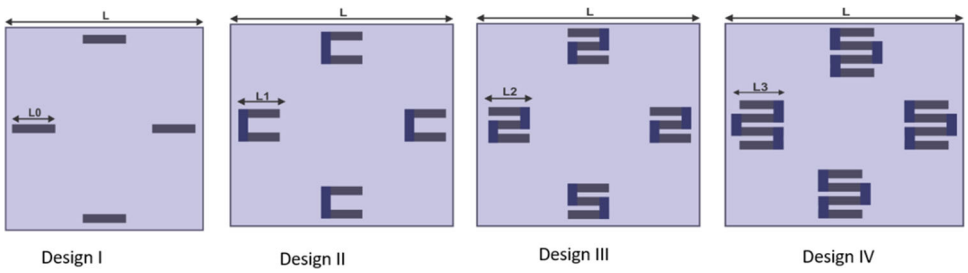

Fig. 9 Four different piezoresistor configurations

Table 1 Sensor characteristics of different meander configurations

Number of turns	SensorSensitivity (mV/kPa)	Non-linearity error (%FSS)
0-turn	23.12	− 0.35
1-turn	25	− 0.27
2-turn	27.82	− 0.33
3-turn	12.56	− 0.38

References

Ali A, Khan A, Ali A, Ahmad M (2017) Pressure-sensitive properties of carbon nanotubes/bismuth sulfide composite materials. Nanomater Nanotechnol 7:1847980417707087

Aqel A, Abou El-Nour KM, Ammar RA, Al-Warthan A (2012) Carbon nanotubes, science and technology part (I) structure, synthesis and characterisation. Arab J Chem 5(1):1–23

Bala S, Khosla M (2018) Comparative study and analysis of CNTFET and tunnel CNTFET. J Nanoelectron Optoelectron 13(3):324–330

Guan T, Yang F, Wang W, Huang X, Jiang B, Zhang D (2016) The design and analysis of piezoresistive Shuriken-structured diaphragm micro-pressure sensors. J Microelectromech Syst 26(1):206–214

Gupta N, Gupta SM, Sharma SK (2019) Carbon nanotubes: synthesis, properties and engineering applications. Carbon Lett 29:419–447

Hossain A, Mian A (2017) Four-terminal square piezoresistive sensors for MEMS pressure sensing. J Sens. https://doi.org/10.1155/2017/6954875

Huang X, Zhang D (2014a) Structured diaphragm with a centre boss and four peninsulas for high sensitivity and high linearity pressure sensors. Micro Nano Lett 9(7):460–463

Huang X, Zhang D (2014b) A high sensitivity and high linearity pressure sensor based on a peninsula-structured diaphragm for low-pressure ranges. Sens Actuat A 216:176–189

Jakati RS, Balavalad KB, Sheeparamatti BG (2016) Comparative analysis of different micro-pressure sensors using comsol multiphysics. In: 2016 International Conference on Electrical, Electronics, Communication, Computer and Optimization Techniques (ICEECCOT) (pp 355–360). IEEE

Katageri AC, Sheeparamatti BG (2015) Carbon nanotube based piezoresistive pressure sensor for wide range pressure sensing applications—a review. Int J Eng Res 4(08):27

Kim JH, Park KT, Kim HC, Chun K (2009) Fabrication of a piezoresistive pressure sensor for enhancing sensitivity using silicon nanowire. In: TRANSDUCERS 2009–2009 International Solid-State Sensors, Actuators and Microsystems Conference (pp 1936–1939). IEEE

Kumar SS, Tanwar A (2020) Development of a MEMS-based barometric pressure sensor for micro air vehicle (MAV) altitude measurement. Microsyst Technol 26(3):901–912

Li C, Cordovilla F, Ocaña JL (2017) The design and analysis of a novel structural piezoresistive pressure sensor for low pressure measurement. Microsyst Technol 23(12):5677–5687

Li C, Cordovilla F, Jagdheesh R, Ocaña JL (2018) Design optimization and fabrication of a novel structural SOI piezoresistive pressure sensor with high accuracy. Sensors 18(2):439

Li C, Zhao L, Ocaña JL, Cordovilla F, Yin Z (2020) Characterization and analysis of a novel structural SOI piezoresistive pressure sensor with high sensitivity and linearity. Microsyst Technol 26(9):2955–2960

Lu J, Lu M, Bermak A, Lee YK (2007) Study of piezoresistance effect of carbon nanotube-PDMS composite materials for nanosensors. In: 2007 7th IEEE Conference on Nanotechnology (IEEE NANO) (pp 1240–1243). IEEE

Meena KV, Mathew R, Sankar AR (2017) Design and optimization of a three-terminal piezoresistive pressure sensor for catheter based in vivo biomedical applications. Biomed Phys Eng Express 3(4):045003

Meti S, Balavald KB, Sheeparmatti BG (2016) MEMS piezoresistive pressure sensor: a survey. Int J Eng Res Appl 6(4 part 1):23–31

Mishra RB, Kumar SS (2019) Mathematical modelling and comparative study of elliptical and circular capacitive pressure microsensor. J Phys 1240(1):012068 ((**IOP Publishing**))

Niu Z, Zhao Y, Tian B (2014) Design optimization of high pressure and high temperature piezoresistive pressure sensor for high sensitivity. Rev Sci Instrum 85(1):015001

Shaby SM, Premi MSG, Martin B (2015) Enhancing the performance of MEMS piezoresistive pressure sensor using germanium nanowire. Procedia Mat 10:254–262

Song P, Si C, Zhang M, Zhao Y, He Y, Liu W, Wang X (2020a) A novel piezoresistive MEMS pressure sensors based on temporary bonding technology. Sensors 20(2):337

Song P, Ma Z, Ma J, Yang L, Wei J, Zhao Y et al (2020b) recent progress of miniature MEMS pressure sensors. Micromachines 11(1):56

Sosa J, Montiel-Nelson JA, Pulido R (2015) Garcia-Montesdeoca JC (2015) Design and optimization of a low power pressure sensor for wireless biomedical applications. J Sens 9:1–13

Suja KJ, Kumar GS, Nisanth A, Komaragiri R (2015) Dimension and doping concentration based noise and performance optimization of a piezoresistive MEMS pressure sensor. Microsyst Technol 21(4):831–839

Tran AV, Zhang X, Zhu B (2017) The development of a new piezoresistive pressure sensor for low pressures. IEEE Trans Industr Electron 65(8):6487–6496

Tran AV, Zhang X, Zhu B (2018) Mechanical structural design of a piezoresistive pressure sensor for low-pressure measurement: a computational analysis by increases in the sensor sensitivity. Sensors 18(7):2023

Wang C, Hou X, Cui M, Yu J, Fan X, Qian J et al (2020) An ultrasensitive and wide measuring range pressure sensor with paper-based CNT film/interdigitated structure. Sci China Mater 63(3):403–412

Xu T, Zhao L, Jiang Z, Guo X, Ding J, Xiang W, Zhao Y (2016) A high sensitive pressure sensor with the novel bossed diaphragm combined with peninsula-island structure. Sens Actuat A 244:66–76

Xu T, Wang H, Xia Y, Zhao Z, Huang M, Wang J et al (2017) Piezoresistive pressure sensor with high sensitivity for medical application using peninsula-island structure. Front Mech Eng 12(4):546–553

Yu H, Huang J (2015) Design and application of a high sensitivity piezoresistive pressure sensor for low pressure conditions. Sensors 15(9):22692–22704

Zhang S, Wang T, Lou L, Tsang WM, Sawada R, Kwong DL, Lee C (2014) Annularly grooved diaphragm pressure sensor with embedded silicon nanowires for low pressure application. J Microelectromech Syst 23(6):1396–1407

Zhao L, Xu T, Hebibul R, Jiang Z, Ding J, Peng N et al (2016) A bossed diaphragm piezoresistive pressure sensor with a

peninsula–island structure for the ultra-low-pressure range with high sensitivity. Meas Sci Technol 27(12):124012

Zhu SE, Krishna Ghatkesar M, Zhang C, Janssen GCAM (2013) Graphene based piezoresistive pressure sensor. Appl Phys Lett 102(16):161904

Zou H, Wang J, Li X (2017) High-performance low-range differential pressure sensors formed with a thin-film under bulk micromachining technology. J Microelectromech Syst 26(4):879–885